STUDIES ON NORMAL AND MICROGRAVITY ANNULAR TWO PHASE FLOWS.

V. Balakotaiah[1], S. S. Jayawardena[2] and L. T. Nguyen[3],
Department of Chemical Engineering, University of Houston, Houston, TX 77204-4792
[1]Bala@uh.edu, [2]Subash@uh.edu, [3]LJN96442@jetson.uh.edu

ABSTRACT

Two-phase gas-liquid flows occur in a wide variety of situations. In addition to normal gravity applications, such flows may occur in space operations such as active thermal control systems, power cycles, and storage and transfer of cryogenic fluids.

Various flow patterns exhibiting characteristic spatial and temporal distribution of the two phases are observed in two-phase flows. The magnitude and orientation of gravity with respect to the flow has a strong impact on the flow patterns observed and on their boundaries. The identification of the flow pattern of a flow is somewhat subjective. The same two-phase flow (especially near a flow pattern transition boundary) may be categorized differently by different researchers.

Two-phase flow patterns are somewhat simplified in microgravity, where only three flow patterns (bubble, slug and annular) have been observed. Annular flow is obtained for a wide range of gas and liquid flow rates, and it is expected to occur in many situations under microgravity conditions. Slug flow needs to be avoided, because vibrations caused by slugs result in unwanted accelerations. Therefore, it is important to be able to accurately predict the flow pattern which exists under given operating conditions.

It is known that the wavy liquid film in annular flow has a profound influence on the transfer of momentum and heat between the phases. Thus, an understanding of the characteristics of the wavy film is essential for developing accurate correlations.

In this work, we review our recent results on flow pattern transitions and wavy films in microgravity.

FLOW PATTERN TRANSITIONS IN MICROGRAVITY

The absence of gravity reduces the number of observed flow patterns to three and it also reduces the number of dimensionless groups needed to characterize two-phase flows by two. For microgravity two-phase flows in a smooth pipe, there are five relevant dimensionless groups:

$$\text{Gas Reynolds number, } Re_{GS} = \frac{\rho_G U_{GS} D}{\mu_G}$$

$$\text{Liquid Reynolds number, } Re_{LS} = \frac{\rho_L U_{LS} D}{\mu_L}$$

$$\text{Weber number, } We_{LS} = \frac{\rho_L U^2_{LS} D}{\sigma}$$

$$\text{Ratio of gas to liquid densities, } = \frac{\rho_G}{\rho_L}$$

$$\text{Ratio of gas to liquid viscosities, } = \frac{\mu_G}{\mu_L}$$

Here, U_{LS} is the superficial velocity of the liquid based on a single phase flow and U_{GS} is the superficial gas velocity. The viscosity, density and surface tension are denoted by μ, ρ and σ, respectively. When the last two ratios are small, the flow pattern transition boundary may be assumed to be a weak function of these two ratios. The number of dimensionless groups may be further reduced to two by combining Re_{LS} and We_{LS} and ignoring the influence of We_{LS} alone.

For microgravity two-phase flows, (using experimental data from various systems) we developed a pair of dimensionless flow pattern transition maps shown in Figs. 1 and 2 (Jayawardena *et al.*, 1997). These maps suggest the importance of Suratman number ($Su = \frac{Re^2_{LS}}{We_{LS}} = \frac{\rho_L \sigma D}{\mu^2_L}$) in determining the transitions between the flow patterns.

<u>BUBBLE-SLUG TRANSITION</u>

The bubble-slug flow pattern transition occurs at a particular value of the ratio (Re_{GS}/Re_{LS}). This transitional value, $(Re_{GS}/Re_{LS})_t$, depends on the Suratman number as given below:

$$(Re_{GS}/Re_{LS})_t = K_1\, Su^{-2/3}. \qquad (1)$$

<u>SLUG-ANNULAR TRANSITION</u>

It is found that when the Suratman number is less than 10^6, slug-annular flow pattern transition occurs at a particular value of the ratio (Re_{GS}/Re_{LS}). This transitional value, $(Re_{GS}/Re_{LS})_t$, was found to depend on the Suratman number as given below:

$$(Re_{GS}/Re_{LS})_t = K_2\, Su^{-2/3}. \qquad (2)$$

When the Suratman number is greater than 10^6, slug-annular flow pattern transition was found to be a function of the gas Reynolds number, Re_{GS}. This transitional value, $(Re_{GS})_t$, was found to depend on the Suratman number as given below:

$$(Re_{GS})_t = K_3\, Su^2. \qquad (3)$$

Experimental data shown in Figs. 1 and 2 suggest the following numerical values:

$K_1 = 464.16,$ (4a)

$K_2 = 4641.6,$ (4b)

$K_3 = 2x10^{-9}.$ (4c)

The Suratman number is determined by the tube diameter and physical properties of the fluid. Thus, the proposed maps can be used to identify the flow pattern for any given two-phase system, even when there are no prior experimental microgravity flow pattern data.

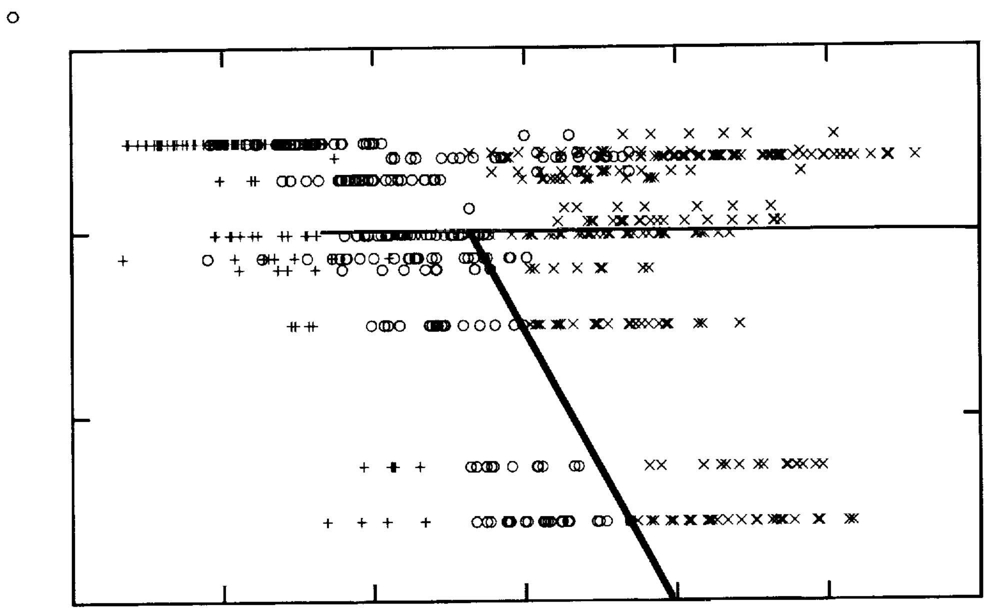

Figure 1. Dimensionless flow pattern map for microgravity two-phase flows. (For slug-annular transition for Su > 10^6 and for bubble-slug transition).

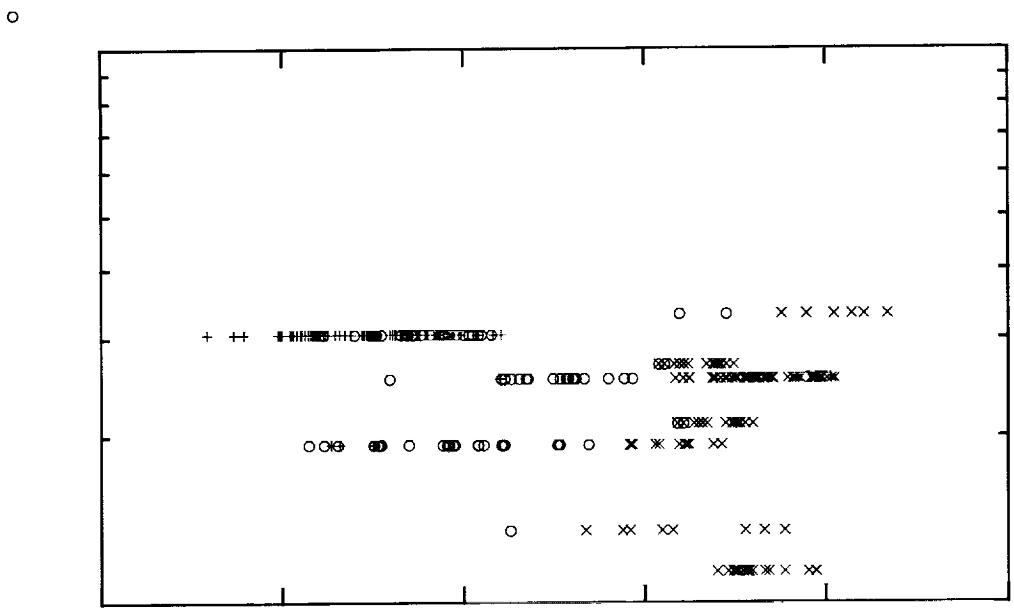

Figure 2. Dimensionless flow pattern map for the slug-annular transition in microgravity two-phase flows (for Su > 10^6).

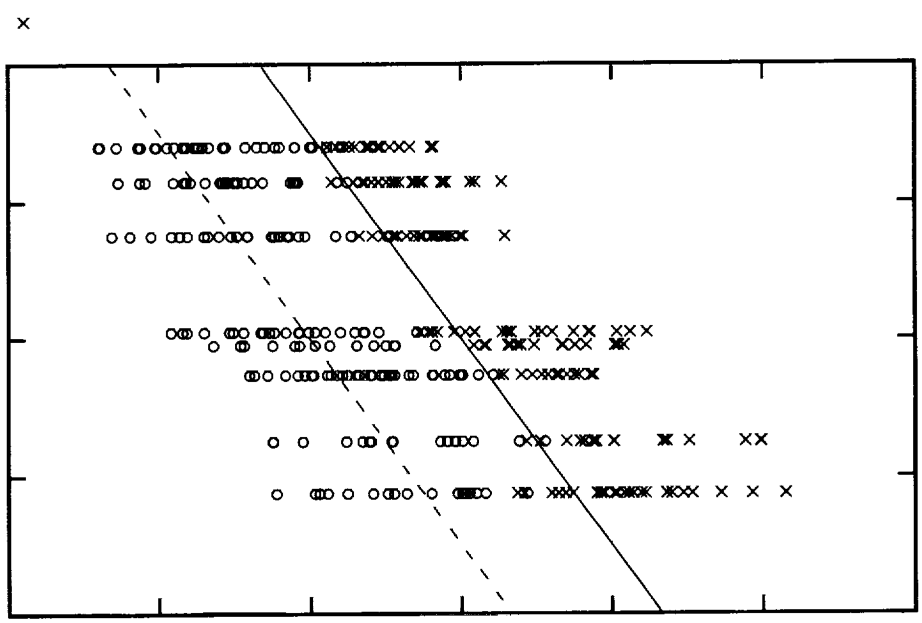

Figure 3. Results of recent microgravity two phase flow tests conducted using various fluids as shown in table 1.

VALIDATION OF PROPOSED MAP

We have collected new flow pattern data on micro-gravity two phase flows. These tests were done using the same test rig used by Bousman (1994), but with different working fluids. The Suratman number was changed by reducing the surface tension and/or by increasing the viscosity using a surfactant and/or glycerin. Figure 3 shows these new data points. The fluid properties and corresponding Suratman numbers are listed in Table 1.

These new experiments confirmed that the slug-annular transition boundary given by Eq. (2) extends to low values of the Suratman number ($10^2 < Su < 10^4$). However, they did not verify the bubble-slug transition boundary. The proposed boundary may not applicable for low Suratman number bubble-slug transitions. On the other hand, due to experimental limitations, the flow visualization was done after 85 pipe diameters. Since the feed section generated annular flow. It is possible that the flow development length was not sufficient to distribute the phases to achieve bubble flow.

When we planned these experiments, our aim was to validate the slug-annular transition for various two phase flows in microgravity and we could do that with flows having Suratman numbers as low as 770.

Table 1. Properties of the fluids used in these tests.

Test Fluid (Wt % of Glycerin)	Su	Properties		
		ρ_L	μ_L	σ
AWG (70)	1800	1181	23.00	64.6
AWGZ (70)	770	1181	23.00	27.0
AWG (60)	8900	1153	10.66	68.9
AWGZ (50)	11000	1125	6.03	27.0
AWG (24)	250000	1056	1.98	72.2
AWG (64)	5400	1164	13.63	68.4
AWG (32)	140000	1077	2.63	71.8
AWGZ (32)	56000	1077	2.63	28.5

(weight percentage of glycerin is given in parentheses)

Key: AW = air-water,
AWG = air-water-glycerin,
AWZ = air-water-Zonyl,
AWGZ = air-water-glycerin-Zonyl,

Units: ρ_L (kg/m^3), μ_L (cP) and σ (dyne/cm),

SYSTEM SPECIFIC, DIMENSIONAL FLOW PATTERN MAPS

Some system specific flow pattern maps (for a given fluid in a selected tube size) are plotted using the two-phase quality vs. mass flow rate. Such maps are useful for single-component, two-phase system. Our flow pattern boundaries may be used to create such system specific flow pattern maps.

The two-phase quality x, is defined as

$$x = \frac{(\rho_G U_{GS})}{(\rho_G U_{GS} + \rho_L U_{LS})}\,. \qquad (5)$$

Combining Eqs. (1), (5) and material balance on the two-phase flow gives the following expressions for the bubble-slug flow pattern boundary for any Suratman number:

$$x_{t,B\text{-}S} = \frac{K_1 \frac{\mu_G}{\mu_L} Su^{-2/3}}{(1 + K_1 \frac{\mu_G}{\mu_L} Su^{-2/3})} \qquad (6)$$

This transitional quality, $x_{t,B\text{-}S}$, is independent of the total mass flow rate.

The criteria for the slug-annular transition depends on the Suratman number of the system. The following expression (from Eqs. (2,) (5) and material balance) gives the slug-annular flow pattern boundary when the Suratman number is smaller than 10^6:

$$x_{t,S\text{-}A} = \frac{K_2 \frac{\mu_G}{\mu_L} Su^{-2/3}}{(1 + K_2 \frac{\mu_G}{\mu_L} Su^{-2/3})} \qquad (Su < 10^6) \quad (7))$$

This transitional quality, $x_{t,S\text{-}A}$, is also independent of the total mass flow rate.

Combining Eqs. (3), (5) and material balance gives the following slug-annular flow pattern boundary when the Suratman number is larger than 10^6:

$$\dot{m}\ x_{t,S\text{-}A} = K_3 \frac{\pi D^3}{4} \frac{\sigma^2 \rho_L{}^2}{\mu_L{}^4}\,\mu \qquad (Su > 10^6) \quad (8)$$

where $\dot{m}$ is the total mass flow rate of the two-phase flow. Equation (8) suggests that it is possible to obtain slug flow at higher values of quality, provided mass flow rate of the two-phase flow is low.

An example of such a single-component, two-phase system is a refrigerant flowing in a tube. In such cases, the total mass flow rate and the quality are the preferred variables to prepare flow pattern maps. Figure 4 shows the flow pattern boundaries on a two-phase quality vs. mass flow rate map, for a selected two-phase system in microgravity.

The bubble flow pattern is observed in an extremely small range of quality. The value for $x_{t,B\text{-}S}$

at that transition is about 0.04%. For most flow conditions in microgravity, annular flow is observed.

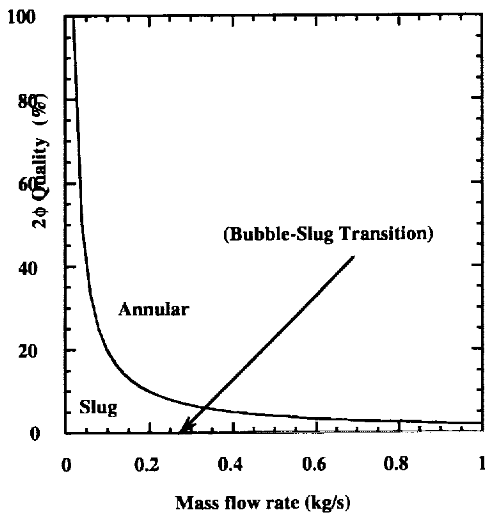

Figure 4. Dimensional, system specific flow pattern map for a single component microgravity two-phase flow. (For refrigerant R134a at 70°F in 25.4 mm ID tube, Su = $4.5\text{x}10^6$)

The system specific flow pattern map for a low ($<10^6$) Suratman number system consists of two straight lines, since the two-phase quality at the flow pattern boundary is independent of the total mass flow rate. A detailed discussion including the critical void fraction of a two component systems is given in Jayawardena and Balakotaiah (1997).

WAVY FILMS IN MICROGRAVITY

We now study characteristics of the wavy films in microgravity annular flows. Bousman (1994) collected data on wavy film profiles in microgravity using air-water, air-water-glycerin and air-water-Zonyl systems. His film thickness data are shown in Fig. 6. Where the dimensionless film thickness is defined as

$$h^+ = \frac{h\,u^*}{\nu_L}, \qquad u^* = \sqrt{\frac{\tau_w}{\rho_L}}. \tag{9}$$

Since wall measured shear stress (τ_w) is not accurate, we estimate τ_w using measured pressure gradient:

$$\tau_w = \left(\frac{dP_G}{dx}\right)\left(\frac{D}{4}\right) \tag{10}$$

where τ_w is the average interfacial stress and D is the tube diameter. The liquid Reynolds number Re_L is defined as

$$Re_L = \left(\frac{4\Gamma}{\nu_L}\right), \tag{11}$$

where Γ is the flow rate in the film per unit perimeter. Since film flow rate is not measured, we approximate Re_L by Re_{LS}, assuming negligible entrainment.

A relationship between h^+ and Re_L is derived by assuming a velocity profile. The following velocity profile is assumed in the film for laminar flow

$$u^+ = y^+. \tag{12}$$

For the turbulent flow, the universal velocity profile

$$u^+ = y^+ \qquad 0 < y^+ < 10$$
$$u^+ = 2.78 \ln y^+ + 3.60 \qquad 10 < y^+ \tag{13}$$

where, u^+ is the dimensionless friction velocity in the film ($u^+ = u/u^*$) is assumed in the liquid film.

These equations gives

$$Re_L = 2\,(h^+)^2 \qquad 0 < h^+ < 10$$
$$Re_L = 3.28\,h^+ + 11.12 \ln h^+ - 88.8 \qquad 10 < h \tag{14}$$

A plot of this equation is shown in Fig. 5 as the solid line. The agreement with data is good. The mean film thickness of normal and microgravity two phase flows are not fundamentally different.

Since we expect the surface tension effects to dominate under microgravity conditions, it is of interest to compare the rms values of the film thickness under normal and microgravity conditions. (Note: The rms film thickness is actually the standard deviation since we subtract the mean film thickness. However, we are following here the literature terminology.)

The rms values of the film thickness fluctuations is normalized using the same length scale defined using the friction velocity u^*, and it is denoted as h^+_{rms}. When h^+_{rms} is plotted against Re_{LS}, it shows a large amount of scatter, partly due to the fact that these data points were collected at different gas velocities ranging from about 5 m/s to about 25 m/s. Experimental observations show that the annular flow liquid film becomes smoother at higher gas flow rates.

The following correlation predicts measured h^+_{rms} values for various flow conditions used in these tests:

$$h^+_{rms} = A\,Re_{LS}^{0.7} \tag{15}$$

Here A is a coefficient which depends only on the gas flow rate. The available data suggests:

$$A = (0.135\text{-}0.0033\,U_{GS}). \tag{16}$$

Figure 6 is a comparison of the predicted h^+_{rms} values with the experimental values. One dilemma here is that our intuition suggests that h^+_{rms} should be affected by the surface tension, where as Eq. (15) indicates the contrary.

Another quantity of interest is the enhancement in the friction factor. Here we compare the friction factor based on the interfacial stress with that of a corresponding single phase gas flow. The friction factor is defined as

$$f_i = \frac{\tau_i}{\frac{1}{2}\rho_G U^2_{GS}} \qquad (17)$$

Asali *et al.* (1985) have analyzed data for co-current down flow and presented a correlation of the form

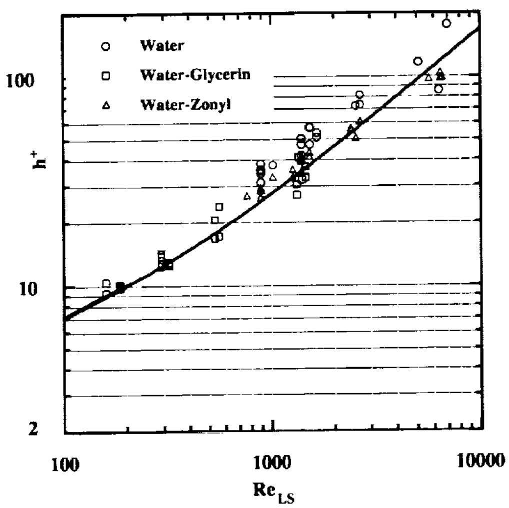

Figure 5. Dependence of normalized liquid film thickness on the liquid Reynolds number for microgravity annular two-phase flow and the comparison with the proposed correlations.

$$\left(\frac{f_i}{f_s} - 1\right) Re^{0.2}_{GS} = 0.45\,(h^+_G - 4) \qquad (18)$$

Here, f_s is the gas phase friction factor that would exist in a smooth tube and

$$h^+_G = \frac{h}{\nu_G}\sqrt{\frac{\tau_w}{\rho_G}} \qquad (19)$$

The microgravity data is shown in Fig. 7 along with the correlation given by Eq. (20). Though the data is more scattered, it is clear that the enhancement in the interfacial friction factor is higher in microgravity than in normal gravity.

If we use all the available micro-gravity data, then the interfacial shear stress can be represented by the following equation:

$$\left(\frac{f_i}{f_s} - 1\right) Re^{0.2}_{GS} = 0.42\, h^{+\;1.18}_G \qquad (20)$$

When we eliminated data points close to the slug annular transition, the following two correlations are obtained.

$$\left(\frac{f_i}{f_s} - 1\right) Re^{0.2}_{GS} = 0.16\, h^{+\;1.3}_G \qquad (21)$$

for water and water-glycerin mixtures and

$$\left(\frac{f_i}{f_s} - 1\right) Re^{0.2}_{GS} = 0.25\, h^{+\;1.3}_G \qquad (22)$$

for water-Zonyl mixture. (Zonyl reduces the surface tension by about a factor three). That indicates that surface tension influences the interfacial structure of the waves.

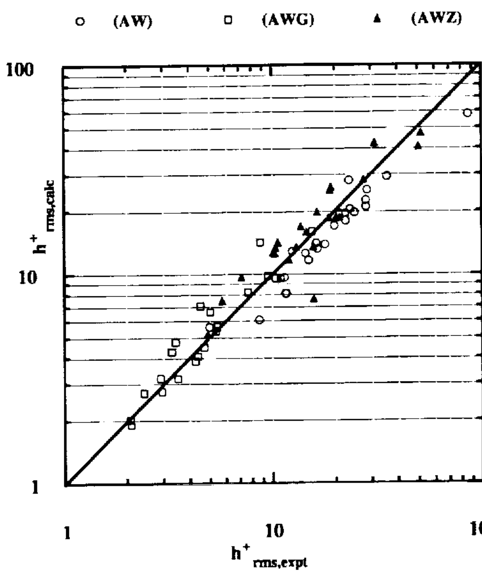

Figure 6. Comparison of calculated h^+_{rms} values with the experimental data.

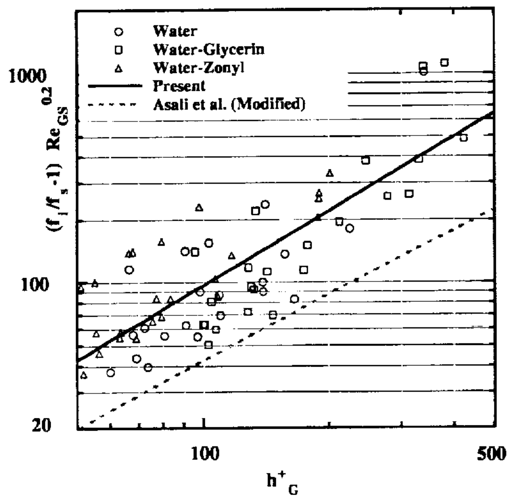

Figure 7. Comparison of the friction factor for the interfacial shear stress in microgravity annular flows with the existing normal gravity annular flow correlation of Asali *et al.* (1985) (Dashed line) with the new correlation (solid line).

CONCLUSIONS AND DISCUSSION

The recently proposed flow pattern map was verified at low Suratman number systems. Experiments confirmed the applicability of the proposed slug-annular flow pattern transition boundary for two phase flow systems with a low Suratman number.

System specific, dimensional flow pattern boundaries can be obtained for microgravity two phase flows. For a wide range of two-phase qualities, slug flow can be observed in such a system if the total mass flow rate is small, provided Suratman number is large. Bubbly flow exists in microgravity only at extremely low two-phase qualities.

The dimensionless parameter affecting the slug-annular transition changes at a Suratman number of about 10^6. Thus, we expect a dramatic change in the mechanism governing the slug-annular transition. It is very important to study liquid film characteristics, pressure gradients and drop entrainment measurements for high Suratman number two-phase flows in microgravity.

When properly non-dimensionalized using the pressure gradient, the mean film thickness of an annular flow depends only on the liquid Reynolds number, irrespective of gravity. Agreement between experimental data and the prediction suggests that entrainment of liquid droplets in microgravity annular flows to be small. This speculation needs experimental validation.

The differences between the normal and microgravity annular liquid films are apparent when we compare the interfacial friction factors. It is found that the friction factor enhancement is higher in microgravity conditions than in normal gravity downward annular flows. In microgravity annular flows, the enhancement to the friction factor is surface tension dependent.

ACKNOWLEDGMENTS

This work is supported by a grant from the NASA-Lewis Research Center (NAG3-1840), a NASA Lewis GSRP grant to Luan Nguyen and the UH-JSC aerospace post-doctoral fellowship program.

REFERENCES

Asali. J. C., Hanratty, T. J. and Andreussi, P., 1985, "Interfacial Drag and Film Height for Vertical Annular Flow", *AIChE J*, **31**, (6), 895.

Bousman, W. S., 1994, "Studies of Two-Phase Gas-Liquid Flow in Microgravity", Ph. D. dissertation, University of Houston.

Jayawardena, S. S., Balakotaiah, V., and Witte, L. C., 1997, "Flow Pattern Transition Maps for Microgravity Two-Phase Flows", *AIChE J.* , **43**, (6), 1637-1640.

Jayawardena S. S. and Balakotaiah, V., 1997 "Studies on Flow Pattern Transitions and Wavy Films in Gas-Liquid Two-Phase Flows in Microgravity", Proceedings of the ASME Winter Annual Meeting, Dallas, Texas, 1997.